ISSN 0016-7029, Geochemistry International, 2018, Vol. 56, No. 12, pp. 1245–1262. © Pleiades Publishing, Ltd., 2018.

Mineralogical and Geochemical Behavior of Sediments Solely Derived from Bundelkhand Granitic Complex, Central India: Implications to Provenance and Source Rock Weathering[1]

S. Kanhaiya, B. P. Singh*, and S. Singh

Center of Advanced Study in Geology, Institute of Science, Banaras Hindu University, Varanasi, 221005 India

**e-mail: drbpsingh1960@gmail.com*

Received June 8, 2017; in final form, November 29, 2017

Abstract—Small rivers commonly drain in a few lithologies making their sediments as a good candidate for investigating provenance and weathering environments. We investigated spatial variation in compositional changes in the sediments of a modern river (Khurar River) from its source to sink for 35 km in Khajuraho area, Madhya Pradesh, India. The Khurar River in its entire course is surrounded by the Bundelkhand granitic complex that provides uniform source to the sediments. The possible physical and chemical controls on the bed-load sediments i.e. grain-size, mineralogy, geochemistry and their climatic control are investigated in detail here. Bed- load sediments of the Khurar River are very coarse to coarse sand-size ranging from −0.63 to 0.80 phi and they are devoid of fine sediments such as clay. The mineralogy of the sediments suggests that they are arkosic in composition. The spatial variation in the chemical composition of the sediments is negligible in the river basin from source to sink in the very coarse to coarse sand size range. The sediments are rich in SiO_2 (≤82.93) and Al_2O_3 (≤11.03 wt %) and they have lower values of TiO_2 (≤0.27), Fe_2O_3 (≤1.49), CaO (≤1.12), MgO (≤0.77), K_2O (≤5.25) and Na_2O (≤3.48 wt %). The trace elements such as Cr (≤66), Co (≤8), Cu (≤19) and Ni (≤12 ppm) have lower values than UCC; but the Pb (≤21) and Rb (≤142 ppm) have higher values than UCC. Lower concentrations of transition elements, such as V, Ni and Cr imply enrichment of felsic minerals in these sediments, a feature also confirmed by the mineralogical study. The high Zn content at some stations suggests anthropogenic contamination in the sediments. A-CN-K ternary plot suggests total alteration of plagioclase resulting in more removal of CaO and Na_2O due to continuous weathering in the catchment area. Also, in this plot, sediments lie near to the albite concentration above the anorthite-albite line with gradual depletion in anorthite indicating that they are the weathering products of albite-enriched parent material. The A-CNK-FM ternary plot shows that all the samples plot close to the feldspar apex indicating higher abundance of feldspars. Further, the CIA (54 to 57), PIA (58 to 64) and CIW (70 to 78) values of the sediment samples suggest low to intermediate weathering environment. Chondrite-normalized pattern of REE (Rare earth elements) exhibits depletion of HREE with weak positive Eu anomaly suggesting low fractionation of the plagioclase feldspar. Thus, the major, trace and rare earth elements geochemistry of the bed-load sediments from the Khurar River suggest that they are derived from the weathering of felsic rocks and the original signatures of the granitic provenance remain there even after weathering under sub-humid climatic conditions in the river basin.

Keywords: River sediments, Sediment geochemistry, Granitic provenance, Khurar River, India

DOI: 10.1134/S0016702918120054

INTRODUCTION

Sediment characteristics are commonly governed by lithology of the provenance, climate, topographic relief, transport energy and hydrodynamics of the depositional environment in a river basin (Sensarma, 2008; Verma et al., 2012; Sharma et al., 2013). Among all, the source area lithology appears to be the most important factor in controlling the sediment mineralogy and geochemistry (Oliva et al., 2003).

Immobile major and trace elements such as Al, Fe, Ti, Th, Sc, Co, Zr and the rare earth elements (REEs) are considered as useful indicators of the provenance (Taylor and McLennan, 1985). It is thought that these elements undergo little geochemical fractionation during denudation processes. However, many post depositional changes such as pedogenesis and diagenesis are able to modify the mobility of certain elements in the deposited sediments (Taylor and McLennan, 1985; McLennan, 1989; White and Blum, 1995; Nesbitt and Young, 1996).

In recent years, several geologists have used chemical characteristics of clastic sediments for the determination of provenance, tectonic setting and weathering in the source terrains (Taylor and McLennan,

[1] The article is published in the original.

1985; Nesbitt and Young, 1996; Gaillardet et al., 1999; Whitemore et al., 2004; Borges and Huh, 2007; Garzanti et al., 2010). Majority of the investigations were focused on bed-load and floodplain sediments of the large rivers may be because of their better global recognition and their large amount of run-off to the oceans (Gaillardet et al., 1999). Since the large rivers drain different rock types, and have long transportation and reworking histories in different climatic zones, the source rock characteristics could not be ascertained unequivocally from sediment geochemistry in majority of the cases (Nesbitt and Young, 1996). Furthermore, the small scale streams are likely to drain fewer lithologies and are representative of weathering environment typical of their basins because geochemical characteristics in small watersheds is only influenced by local meteorological, geological, biological, and anthropogenic complexities (White and Blum, 1995), and better constrain the nature of source materials (Sensarma et al., 2008). Thus, the sediment geochemistry of small-scale watersheds is more suitable for determining the provenance and influence of climate on weathering. The sediment characterizations of a small-scale watershed by Sensarma et al. (2008) are altogether different from the present study because of the diverse compositions of the two catchments where they investigated the sediments derived from the Deccan Basalt and we have investigated the sediments derived from the Bundelkhand granitic complex.

Condie (1991) has suggested that the rare earth elements (REE) show a REE pattern comparable to that of their average source by the time they enter the suspended load of rivers. Contrary to that Sholkovitz (1988) has shown that river-borne sediments commonly have strongly depleted HREE patterns relative to shale. Thus, the influence of lithology on the REE concentrations in river sediments is not well understood. In order to understand the spatial variation in the sediment geochemistry exclusively derived from the granitic source rock and the level of weathering in the source terrain, we studied the sediments of the Khurar River, a major upland tributary of the Ken River in Khajuraho area, Madhya Pradesh, India.

In this paper, we have investigated the textural, mineralogical, major, trace and rare earth elements (REE) composition of the bed load sediments collected from the Khurar River, Madhya Pradesh, India to interpret the major oxide, trace element and REE distribution patterns and their compatibility with the uniform granitic source occupying the river basin. Also, we have inferred the fractionation pattern in the chemical composition of the sediments from its source and the impact of sub-humid climate prevailing in the river basin on the weathering intensity.

GEOMORPHOLOGY AND CLIMATE

The Khurar River is the main tributary of Ken River, a tributary of river Yamuna. It is a small river with its total length about 35 km that originates from the village Saddupura near Khajuraho town (Lat. 24°48′3.5″ N and Long. 79°52′59.6″ E) and confluences with Ken river at Ghadiyal pond, near Renneh fall in the area of Panna tiger reserve (Lat. 24°54′13.9″ N and Long. 80°2′6″ E). It flows from SW to NE direction in the Chhatarpur district, Madhya Pradesh, India occupying a central position in the plateau of Bundelkhand (Figs. 1, 2). The width of the river is ranging from 5 to 15 meter and average velocity is 2.5 meter/second. The river deposits small (2–4 m large) braid-bars in the middle of the channel that deposits sediments during monsoon season mainly.

The river flows exclusively on Archean rocks of Bundelkhand craton. The Bundelkhand Craton occupies the north-central region of the Indian sub-continent, and is situated between 24°11′ to 26°27′ N and 78°10′ to 81°24′ E, covering about 26.000 km^2. The Bundelkhand craton is composed mainly of granitic rocks (Kaur et al., 2014) of Archean to Palaeoproterozoic age (Figs. 1a, 1b), with a few occurrences of supracrustal rocks and older crust (Kumar et al., 2010). Rb–Sr radiometric dates of granite samples from different area of the Bundelkhand craton by Crawford (1970) suggests an average age of 2550 Ma for these rocks. Using the same technique, Sarkar et al. (1984) dated these granites occurring in three phases in the SW part of the craton and suggested an age of 2402 to 2246 Ma for them. Recently, Verma et al. (2016) found 2.25 Ga age of the Bundelkhand granites using U–Pb zircon dating technique.

The climate of the study area is sub-humid with the normal annual rainfall about 1068 mm. The area receives maximum rainfall during south-west monsoon period. About 90.2% of the annual rainfall is received during June to September. Only 9.8% of the annual rainfall takes place from October to May period. The normal maximum temperature of the area during the month of May is 42.3°C and minimum during the month of January is 7.1°C. During the south-west monsoon season the relative humidity generally exceeds 88% (August month) and the rest of the year is drier. The driest part of the year is the summer season, when relative humidity is less than 30% and the May is the driest month of the year.

SAMPLING AND ANALYTICAL METHODS

A total of forty eight bed-load samples from the entire course of the river were collected for further analyses. The sediment samples were washed with dilute H_2O_2 to remove possible organic matter and then air dried. After conning and quartering, grain size analyses of the collected samples have been carried out using sonic shaker in the Sedimentology laboratory of Banaras Hindu University, India. The samples were powdered to –60 mesh size in hard steel mortar and pestle specially designed for geochemical analysis. To

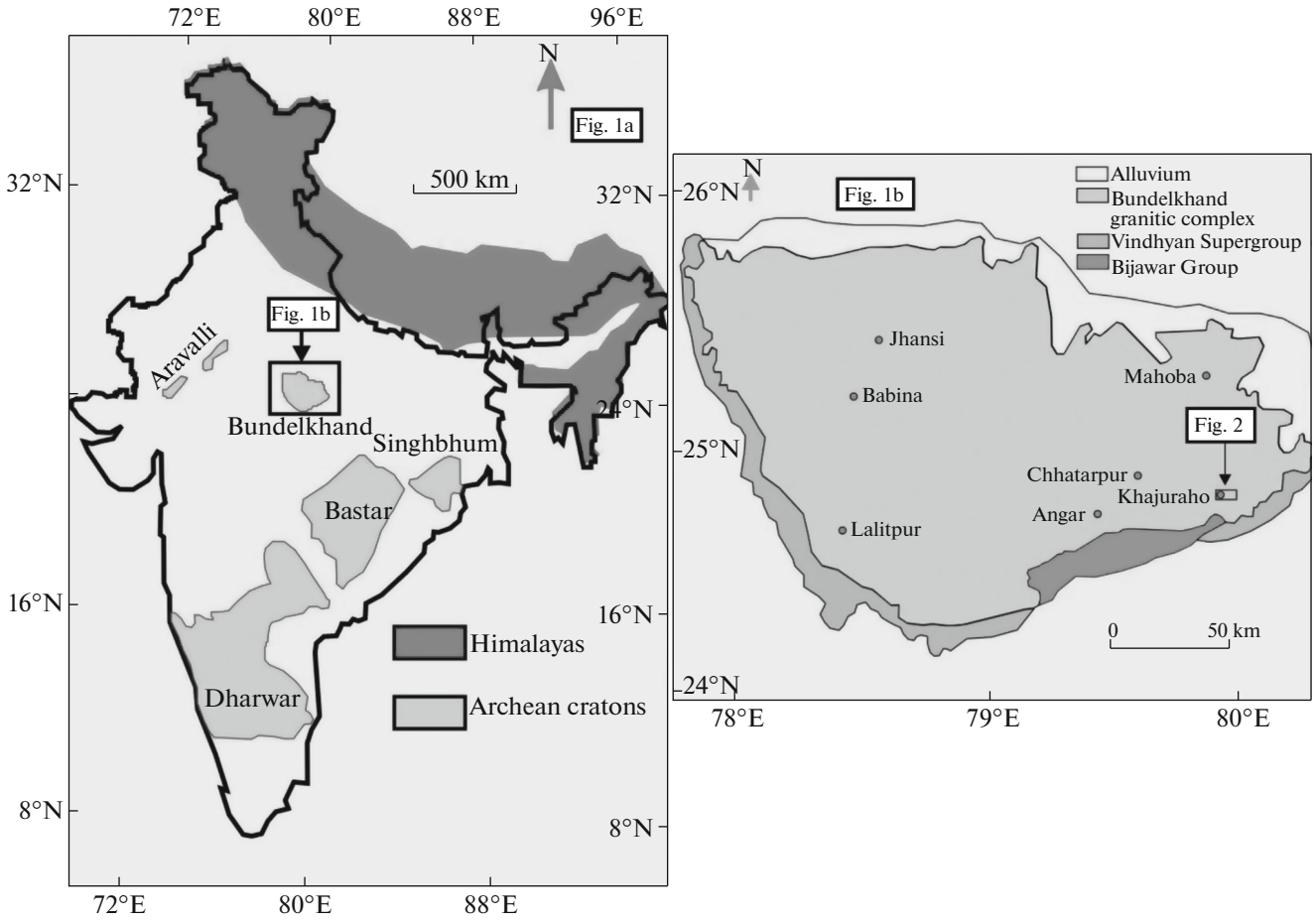

Fig. 1. (a and b) Geological map of India showing Archean cratons and simplified map of Bundelkhand craton (modified after Saha et al., 2011; Verma et al., 2016).

ensure homogenization, the −60 mesh sample powders were rolled several times on a large clean butter paper. After coning and quartering, about 50 g of the sample powder was taken and ground to −200 mesh size in an agate mortar. These well homogenized samples were stored in sample vials for chemical analysis. At every step, care was taken to keep contamination to a minimum level.

The pellets were prepared and analyzed for major and minor elements using Wavelength dispersive XRF technique (SiemensSRS3000) at Wadia Institute of Himalayan Geology, Dehradun, India. Details of the pellet preparation method are available in Stork et al. 1987 and Saini et al. 2000. The precision and accuracy of the sample preparation and instrumental performance were checked using several international reference standards of soil and sediments, e.g., SO-1, GSS-1, GSS-4, GXR-2, GXR-6, SCO-1, SGR-1, SDO-1, MAG-1, GSD-9, GSD-10, GSR-6 and BCS-267. The accuracy of measurement is better than 2–5% and precision <2% (see Purohit et al., 2010 for details). Trace elements, including rare earth elements (REE), were analyzed by ICP-MS (Perkin Elmer SCIEX ELAN DRC), also at WIHG, Dehradun, India after digestion of the samples in Teflon crucibles using a mixture of HF + HNO_3 + $HClO_4$ acids by the method suggested for the preparation of the 'solution-B' method by Shapiro and Brannock (1962). The details of the procedure adopted for the REE determination are given in Khanna et al. (2009). Several USGS standards (SGR-1, MAG-1 and SCo-1) and a few in-house standards were used for calibration. Precision for the ICP-MS analyses obtained is 95%.

RESULTS

Since texture is one of the key parameters that control geochemistry of the sediments, the textural parameters were calculated based on grain size analyses and they are presented in Table 1. The minerals phases present in the samples were identified based on XRD analysis. The major, trace and REE concentrations of the sediments are given in Table 2, while the elemental correlations are presented in Table 3.

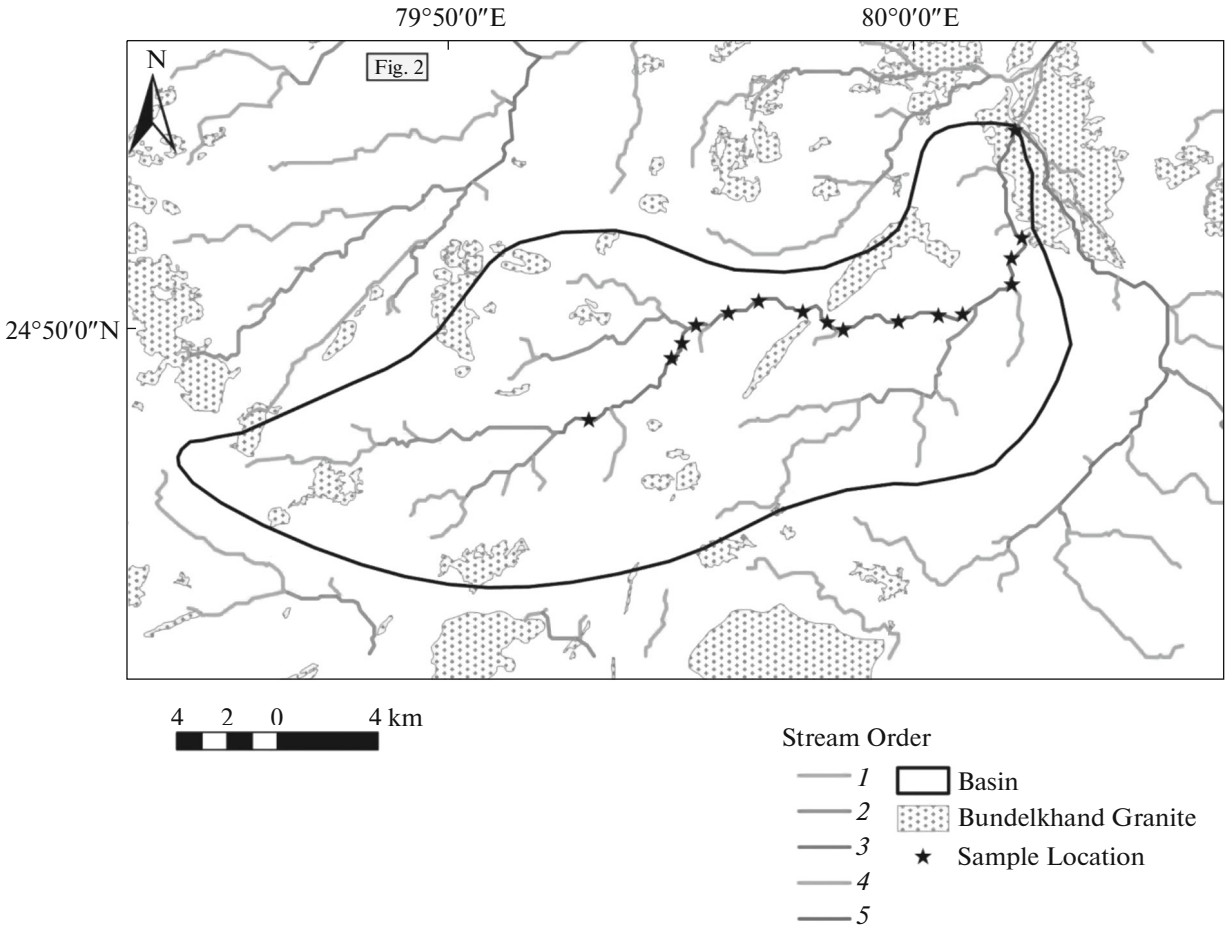

Fig. 2. Map showing Khurar River basin, sampling locations and outcrops of Bundelkhand granite in the area.

Texture and Mineralogy

Bulks of the sediments are very coarse to coarse sand category in the studied samples. All the sediments of Khurar River are characterized by the rolling process of deposition. In general, the samples show poor sorting in the beginning (near to origin) followed by moderate sorting to moderately well sorting at last site where the river confluences with the Ken River. The change of sorting from poorly sorted to moderately sorted and moderately well sorted suggests that the winnowing and selective sorting is possible even in the small river depending upon the hydrodynamic condition of the river (Kanhaiya and Singh, 2014). Most of the samples show positively skewed skewness values because of the domination of the very coarse and coarse fractions. Further, majority of the samples show mesokurtic kurtosis values with very few leptokurtic values (Table 1).

The XRD data of bed-load sediments of the Khurar River show that the primary felsic minerals present are quartz, microcline, albite, orthoclase, and oligoclase. The biotite only occurs as a mafic mineral in these sediments. The clay minerals are almost absent in the studied sediment samples due to prevalence of the coarse fractions in them.

In the $\log(Na_2O/K_2O)$ vs. $\log(SiO_2/Al_2O_3)$ following Pettijohn et al. (1972) and $\log(FeO/K_2O)$ vs. $\log(SiO_2/Al_2O_3)$ following Herron (1988) plots (Figs. 3a, 3b) most of samples occupy the arkosic field.

Major Oxides Geochemistry

The chemical analysis of the studied sediment samples reveals that the concentrations of the major element are compatible with the observed mineralogical data and there is negligible variation in the geochemistry data from source to sink (Table 2). The SiO_2 content in sediments, ranging from 69.96 to 82.73 wt %, is higher and Al_2O_3, ranging from 8.42 to 13.12 wt %, is lower than the Bundelkhand granite. There is strong negative correlation between SiO_2 and major oxides such as, Al_2O_3, TiO_2, Fe_2O_3, MgO, CaO and Na_2O (Fig. 4, Table 3). The TiO_2 concentrations are relatively low and uniform (0.11 to 0.27 wt %) (Table 2). The CaO concentrations vary significantly from 0.31 to 1.12 wt % and the MgO content is varying consider-

Table 1. Textural parameters of the bed load sediments of the Khurar River, Central India

Sample	Size distribution	Mean grain size	Sorting	Skewness	Kurtosis
K 1	Bi-modal	Very coarse sand	Poorly sorted	Fine skewed	Mesokurtic
K2	Bi-modal	Very coarse sand	Poorly sorted	Fine skewed	Mesokurtic
K3	Bi-modal	Coarse sand	Poorly sorted	Near symmetrical	Leptokurtic
K4	Uni-modal	Very coarse sand	Moderately sorted	Coarse skewed	Very leptokurtic
K5	Bi-modal	Very coarse sand	Moderately sorted	Near symmetrical	Mesokurtic
K6	Bi-modal	Very coarse sand	Moderately sorted	Near symmetrical	Platykurtic
K7	Bi-modal	Very coarse sand	Moderately sorted	Near symmetrical	Mesokurtic
K8	Uni-modal	Coarse sand	Moderately sorted	Fine skewed	Mesokurtic
K9	Bi-modal	Very coarse sand	Moderately sorted	Near symmetrical	Mesokurtic
K10	Bi-modal	Coarse sand	Moderately sorted	Coarse skewed	Leptokurtic
K11	Bi-modal	Coarse sand	Moderately sorted	Coarse skewed	Mesokurtic
K12	Uni-modal	Coarse sand	Moderately sorted	Near symmetrical	Leptokurtic
K13	Bi-modal	Very coarse sand	Moderately sorted	Near symmetrical	Mesokurtic
K14	Bi-modal	Coarse sand	Moderately sorted	Coarse skewed	Leptokurtic
K15	Uni-modal	Coarse sand	Moderately sorted	Coarse skewed	Platykurtic
K16	Uni-modal	Coarse sand	Moderately well sorted	Fine skewed	Mesokurtic

ably from 0.09–0.73%. The Na_2O ranges from 1.91–3.48 wt % while K_2O ranges from 4.46–5.25 wt %. The K_2O/Na_2O ratio (1.09 to 2.55) and Al_2O_3/TiO_2 ratio (48.59 to 82.72) are high in the studied sediment samples. CaO concentration is higher than the Bundelkhand granite 0.24 wt % (Table 2) showing variations in degree of weathering of source rock or precipitation of $CaCO_3$. The MnO and P_2O_5 contents are strongly depleted with more or less no significant difference in its contents among the studied samples. The LOI values reflecting the occurrence of clay minerals and hydroxides are more or less negligible in the studied samples. Low values of the MgO are consistent with the poor occurrence of clay minerals.

A–CN–K Diagram

An useful way to evaluate the chemical weathering trend is A–CN–K ternary plot (Nesbitt and Young, 1984; Nesbitt, 2003). At initial stage of weathering A–CN–K plots tend to be parallel to the A–CN line because Na_2O and CaO are leached out from the earlier dissolved plagioclase. Moderate weathering leads to the total destruction of plagioclase resulting in more removal of CaO and Na_2O and the points plot more close to A-K boundary. Intense weathering removes K in preference to Al from the K-feldspar; as a result the trend is redirected to Al_2O_3 apex. Further, the CIA indicates the degree of chemical weathering and is defined as $[Al_2O_3/(Al_2O_3 + CaO + Na_2O + K_2O) \times 100]$ in molecular proportions, where CaO is from the silicates only (Nesbitt and Young, 1984; Nesbitt, 2003). The CIA of sediments is, commonly, about 50 for first cycle sediments dominantly derived from physically weathered igneous rocks and it tends to increase as

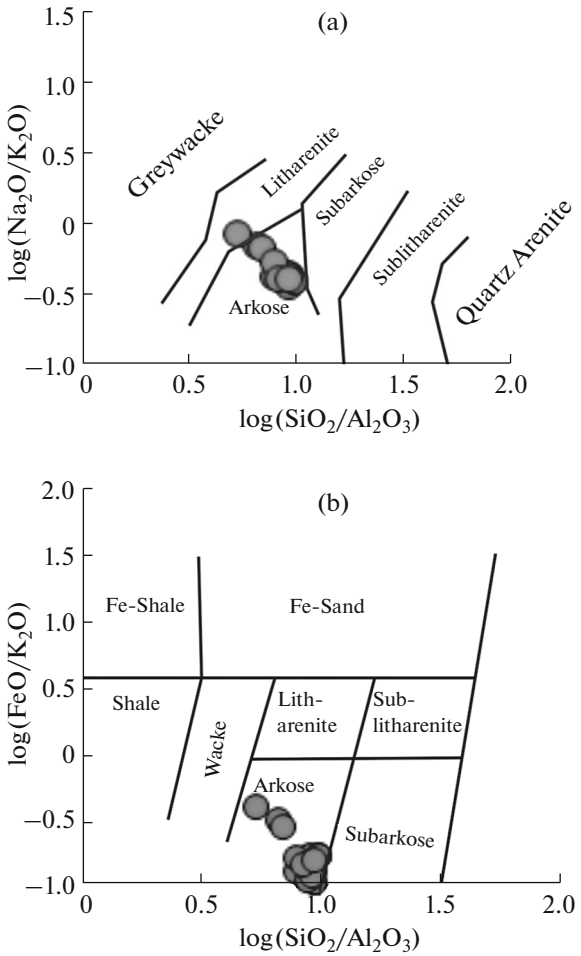

Fig. 3. (a) Plot of the sediments in log Na_2O/ K_2O vs. log SiO_2/Al_2O_3 diagram (Pettijohn et al., 1972). (b) Plot of the sediments in log F_2O/K_2O vs. log SiO_2/Al_2O_3 diagram (Herron, 1988). Note that all the sediments plot in arkose field in both the plots.

Table 2. Major, trace and rare earth element compositions of the Khurar River sediments. Also given compositions of UCC (Rudnick and Gao, 2003) and Bundelkhand granite (BG) (Pati et al., 2015) for comparison

	K1	K2	K3	K4	K5	K6	K7	K8	K9	K10	K11	K12	K13	K14	K15	K16	UCC	BG
Major oxide, wt %																		
SiO_2	73.33	75.41	78.39	82.00	82.55	80.64	82.73	82.20	81.44	79.40	81.42	82.38	82.42	79.93	69.96	81.93	66.60	71.60
Al_2O_3	11.03	10.93	10.00	8.91	8.72	9.13	8.45	9.11	9.10	10.07	8.74	8.89	8.42	9.49	13.12	8.81	15.40	13.30
TiO_2	0.22	0.18	0.15	0.14	0.11	0.11	0.11	0.14	0.11	0.18	0.13	0.12	0.13	0.14	0.27	0.14	0.64	0.23
Fe_2O_3	1.49	1.34	0.72	0.76	0.51	0.57	0.78	0.81	0.71	0.81	0.64	0.63	0.84	0.76	1.95	0.75	5.04	1.94
MnO	0.026	0.029	0.018	0.019	0.007	0.007	0.043	0.018	0.020	0.014	0.013	0.007	0.013	0.023	0.027	0.012	0.1	0.03
MgO	0.73	0.45	0.11	0.16	0.11	0.12	0.14	0.22	0.16	0.19	0.12	0.09	0.12	0.17	0.77	0.16	2.48	0.98
CaO	1.12	0.82	0.41	0.36	0.31	0.35	0.35	0.42	0.43	0.52	0.44	0.32	0.46	0.74	0.67	0.38	3.59	0.24
Na_2O	3.48	3.30	2.42	2.12	2.08	2.23	1.91	2.13	2.20	2.77	1.97	1.93	2.01	2.25	4.30	2.03	3.27	3.27
K_2O	4.59	4.50	5.25	4.49	4.51	4.85	4.46	4.65	4.66	4.83	4.71	4.93	4.70	5.04	4.69	4.60	2.8	5.80
P_2O_5	0.17	0.16	0.14	0.05	0.03	0.05	0.04	0.05	0.04	0.04	0.05	0.03	0.03	0.03	0.04	0.03	0.15	0.06
LOI	2.19	2.44	1.11	1.16	0.84	0.78	1.09	1.11	1.13	1.55	0.95	0.89	1.25	1.33	2.57	1.07	NA	2.4
Total	96.19	97.12	97.61	99.01	98.94	98.06	99.01	99.75	98.87	98.82	98.23	99.33	99.14	98.57	95.80	98.84	100	33.3
Trace element, ppm																		
Ba	603.00	694.00	791.00	701.00	684.00	730.00	692.00	722.00	698.00	763.00	692.00	816.00	763.00	782.00	824.00	729.00	628.00	420.00
Co	5.00	7.00	6.00	8.00	3.00	5.00	6.00	6.00	6.00	5.00	7.00	5.00	7.00	6.00	6.00	6.00	17.30	4.40
Cr	66.00	51.00	50.00	18.00	18.00	37.00	32.00	7.00	18.00	7.00	56.00	14.00	17.00	14.00	29.00	16.00	92.00	12.00
Cu	8.00	9.00	4.00	4.00	5.00	5.00	5.00	6.00	4.00	6.00	6.00	5.00	6.00	6.00	19.00	5.00	28.00	–
Ga	13.00	13.00	11.00	11.00	10.00	9.00	11.00	10.00	10.00	12.00	9.00	10.00	10.00	11.00	15.00	11.00	17.50	–
Nb	11.00	8.00	5.00	5.00	5.00	4.00	4.00	5.00	4.00	7.00	6.00	4.00	4.00	4.00	12.00	6.00	12.00	–
Ni	12.00	7.00	6.00	10.00	9.00	7.00	12.00	8.00	9.00	7.00	9.00	8.00	7.00	7.00	9.00	8.00	47.00	13.30
Pb	24.00	25.00	25.00	22.00	22.00	22.00	22.00	22.00	21.00	23.00	23.00	22.00	21.00	24.00	24.00	21.00	17.00	–
Rb	164.00	142.00	178.00	148.00	148.00	159.00	149.00	155.00	158.00	162.00	160.00	161.00	151.00	160.00	147.00	149.00	84.00	211.00
Sc	3.90	3.50	1.10	BDL	BDL	BDL	2.10	1.40	1.80	BDL	BDL	2.00	1.10	4.00	1.40	1.00	14.00	3.70

Table 2. (Contd.)

	K1	K2	K3	K4	K5	K6	K7	K8	K9	K10	K11	K12	K13	K14	K15	K16	UCC	BG
Sr	143.00	134.00	140.00	115.00	121.00	123.00	115.00	117.00	121.00	138.00	120.00	141.00	157.00	156.00	130.00	148.00	320.00	86.6
Th	20.00	24.00	23.00	11.00	10.00	12.00	9.00	11.00	7.00	18.00	16.00	12.00	5.00	16.00	19.00	7.00	10.50	–
V	23.00	21.00	12.00	12.00	6.00	7.00	8.00	12.00	9.00	14.00	8.00	9.00	13.00	10.00	25.00	9.00	2.70	–
Y	18.00	20.00	17.00	14.00	13.00	13.00	13.00	14.00	13.00	17.00	15.00	13.00	13.00	15.00	22.00	13.00	21.00	–
Zn	16.00	11.00	2.00	4.00	BDL	BDL	BDL	3.00	2.00	2.00	BDL	BDL	BDL	2.00	27.00	2.00	67.00	35.60
Zr	85.00	143.00	116.00	65.00	54.00	66.00	58.00	72.00	56.00	100.00	74.00	51.00	57.00	72.00	195.00	58.00	193.00	289.00
REE (ppm)																		
La	47.6	30.4	17.2	17.8	14.1	11.5	14.5	20.8	11.2	28.5	20.6	14.1	13.9	23.4	55.4	16.9	31	25
Ce	86	54.5	33	38	23.5	21.6	33.5	39	23.9	50.1	38.6	28.3	28.6	40.1	103	30.6	63	49.9
Nd	28.7	20.6	11.6	11.5	8.3	7.7	9.5	13.8	7.4	18	12.5	9.3	10.5	13.4	36.2	11	27	17.8
Sm	4.38	3.79	1.93	1.94	1.31	1.33	1.66	2.21	1.33	2.94	2.08	1.49	1.77	2.11	6.28	1.83	4.7	3.81
Eu	0.9	0.83	0.57	0.55	0.42	0.48	0.53	0.61	0.49	0.72	0.58	0.5	0.55	0.64	1.36	0.55	1	0.66
Gd	3.14	2.87	1.43	1.42	1.03	1.07	1.29	1.65	1	2.14	1.54	1.16	1.25	1.54	4.78	1.29	4	4.29
Dy	1.74	2.47	1.22	1	0.83	0.92	1	1.26	0.8	1.5	1.06	0.83	0.82	1.07	3.83	0.91	3.9	–
Er	0.99	1.51	0.75	0.57	0.49	0.57	0.61	0.72	0.48	0.88	0.6	0.48	0.48	0.61	2.28	0.53	2.3	–
Yb	0.93	1.44	0.75	0.57	0.44	0.53	0.54	0.66	0.46	0.84	0.6	0.45	0.47	0.54	2.1	0.5	1.96	1.82
Lu	0.15	0.23	0.13	0.09	0.07	0.09	0.09	0.11	0.07	0.14	0.1	0.07	0.08	0.09	0.33	0.08	0.31	0.3
Eu/Eu*	0.68	0.67	0.64	0.62	0.57	0.64	0.64	0.64	0.66	0.66	0.63	0.63	0.66	0.69	0.85	0.64	0.70	0.55
Th/Cr	0.30	0.47	0.46	0.61	0.56	0.32	0.28	1.57	0.39	2.57	0.29	0.86	0.29	1.14	0.66	0.44	0.11	–
La/Sc	12.21	8.69	15.64	–	–	–	6.90	14.86	6.22	–	–	7.05	12.64	5.85	39.57	16.90	2.21	6.76
Th/Sc	5.13	6.86	20.91	–	–	–	4.29	7.86	3.89	–	–	6.00	4.55	4.00	13.57	7.00	0.75	–
Zr/Y	4.72	7.15	6.82	4.64	4.15	5.08	4.46	5.14	4.31	5.88	4.93	3.92	4.38	4.80	8.86	4.46	9.19	–
La/Sm	10.87	8.02	8.91	9.18	10.76	8.65	8.73	9.41	8.42	9.69	9.90	9.46	7.85	11.09	8.82	9.23	6.60	6.56
La/Yb	51.18	21.11	22.93	31.23	32.05	21.70	26.85	31.52	24.35	33.93	34.33	31.33	29.57	43.33	26.38	33.80	15.82	13.74

Table 3. Correlation coefficient among chemical parameters for the sediments of the Khurar River, Central India

	SiO_2	Al_2O_3	TiO_2	Fe_2O_3	MnO	MgO	CaO	Na_2O	K_2O	P_2O_5	Ba	Co	Cr	Cu	Ni	Pb	Rb	Sr	Th	Zr	La	Ce	Nd	Sm	Eu	Gd	Dy	Yb
SiO_2	1.0																											
Al_2O_3	−1.0	1.0																										
TiO_2	−0.9	0.9	1.0																									
Fe_2O_3	−0.9	0.9	0.9	1.0																								
MnO	−0.4	0.4	0.3	0.5	1.0																							
MgO	−0.9	0.9	0.9	1.0	0.5	1.0																						
CaO	−0.8	0.7	0.7	0.7	0.4	0.8	1.0																					
Na_2O	−1.0	1.0	0.9	0.9	0.4	0.9	0.7	1.0																				
K_2O	0.0	0.1	0.0	−0.2	−0.3	−0.3	−0.1	−0.1	1.0																			
P_2O_5	−0.6	0.5	0.4	0.4	0.3	0.5	0.7	0.5	0.0	1.0																		
Ba	−0.1	0.2	0.1	0.0	−0.2	−0.2	−0.3	0.0	0.6	−0.4	1.0																	
Co	0.0	0.0	0.1	0.2	0.3	0.0	0.1	0.0	−0.1	0.1	0.0	1.0																
Cr	−0.5	0.3	0.3	0.4	0.3	0.4	0.5	0.4	0.0	0.8	−0.4	0.1	1.0															
Cu	−0.8	0.9	0.9	0.9	0.3	0.8	0.5	0.9	−0.1	0.1	0.3	0.0	0.2	1.0														
Ni	−0.1	0.0	0.1	0.2	0.5	0.4	0.2	0.1	−0.6	0.1	−0.6	0.0	0.3	0.1	1.0													
Pb	−0.7	0.7	0.6	0.5	0.4	0.5	0.6	0.6	0.4	0.7	0.1	0.1	0.6	0.4	−0.2	1.0												
Rb	0.0	0.0	−0.1	−0.3	−0.2	−0.2	0.0	−0.1	0.8	0.3	0.2	−0.2	0.2	−0.3	−0.3	0.3	1.0											
Sr	−0.2	0.1	0.2	0.1	−0.2	0.1	0.4	0.1	0.5	0.1	0.4	0.0	0.0	0.1	−0.4	0.2	0.2	1.0										
Th	−0.7	0.7	0.6	0.5	0.3	0.5	0.6	0.7	0.3	0.7	0.1	0.0	0.6	0.4	−0.2	1.0	0.3	0.1	1.0									
Zr	−0.9	0.9	0.8	0.8	0.4	0.7	0.5	0.9	0.1	0.4	0.3	0.2	0.3	0.8	−0.2	0.7	−0.1	0.1	0.7	1.0								
La	−0.9	0.9	1.0	0.9	0.4	1.0	0.8	0.9	−0.1	0.4	0.0	0.0	0.4	0.9	0.3	0.6	−0.1	0.2	0.6	0.8	1.0							
Ce	−0.9	0.9	1.0	0.9	0.5	1.0	0.8	0.9	−0.1	0.4	0.0	0.1	0.4	0.9	0.3	0.6	−0.1	0.1	0.6	0.8	1.0	1.0						
Nd	−0.9	0.9	1.0	1.0	0.4	1.0	0.8	1.0	−0.1	0.4	0.0	0.0	0.3	0.9	0.2	0.6	−0.1	0.2	0.6	0.8	1.0	1.0	1.0					
Sm	−0.9	0.9	1.0	1.0	0.4	0.9	0.7	1.0	−0.1	0.4	0.1	0.1	0.3	0.9	0.2	0.6	−0.2	0.1	0.6	0.9	1.0	1.0	1.0	1.0				
Eu	−0.9	0.9	1.0	1.0	0.4	0.9	0.7	0.9	−0.1	0.3	0.2	0.1	0.3	0.9	0.1	0.6	−0.2	0.1	0.6	0.9	1.0	1.0	1.0	1.0	1.0			
Gd	−0.9	1.0	1.0	1.0	0.4	0.9	0.7	1.0	−0.1	0.4	0.1	0.1	0.3	0.9	0.2	0.6	−0.2	0.1	0.6	0.9	1.0	1.0	1.0	1.0	1.0	1.0		
Dy	−0.9	0.9	0.9	0.9	0.4	0.9	0.6	0.9	−0.1	0.3	0.2	0.1	0.3	0.9	0.0	0.6	−0.3	0.0	0.6	1.0	0.9	0.9	0.9	1.0	1.0	1.0	1.0	
Yb	−0.9	0.9	0.9	0.9	0.4	0.8	0.5	0.9	−0.1	0.4	0.2	0.1	0.3	0.9	0.0	0.6	−0.3	0.0	0.6	1.0	0.9	0.9	0.9	0.9	0.9	1.0	1.0	1.0

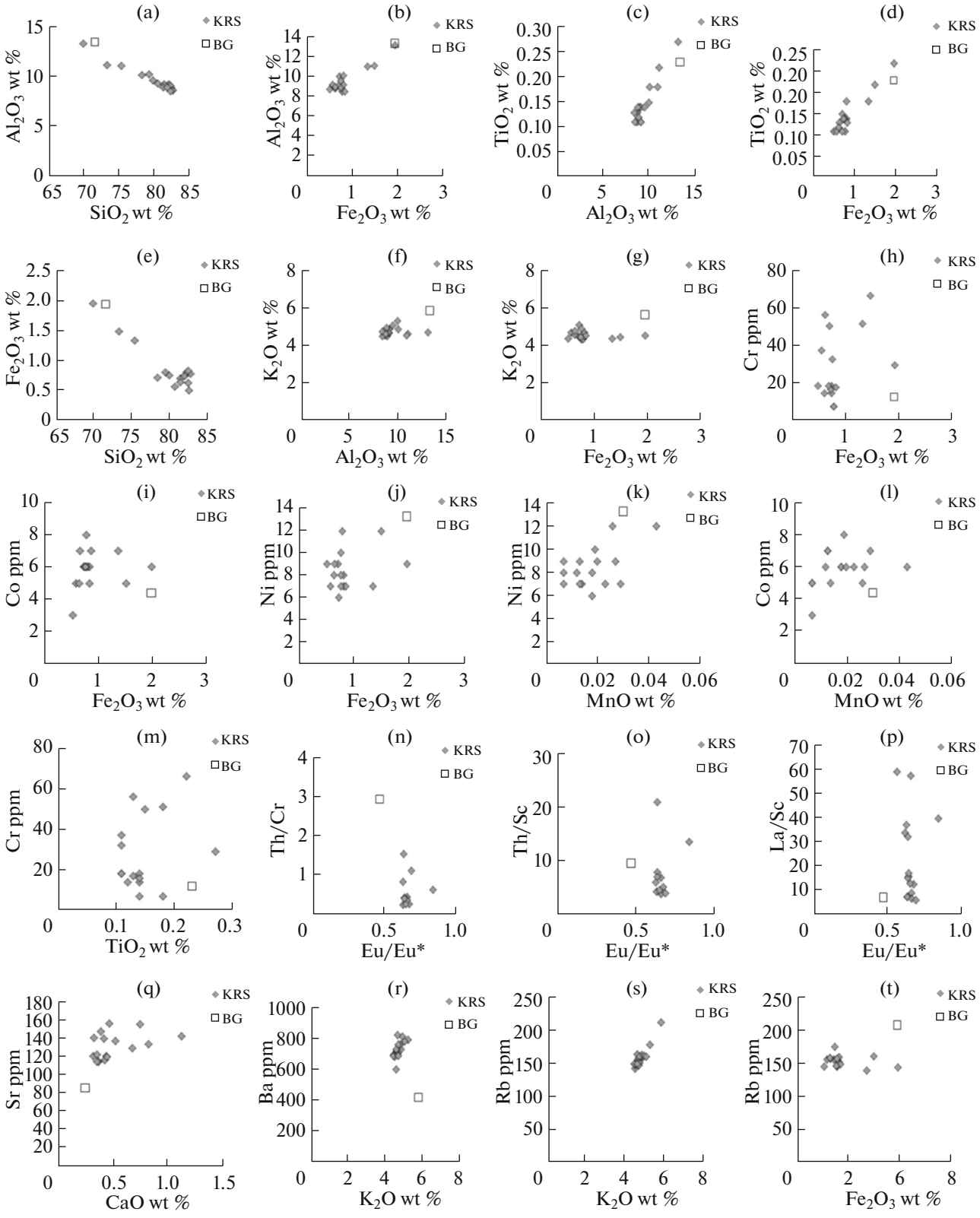

Fig. 4. Binary plots showing relations among different major oxides and trace elements for the Khurar River bed load samples. Compositions of the Bundelkhand granite (BG) (data after Pati et al., 2015) are plotted for comparison. For details, see text.

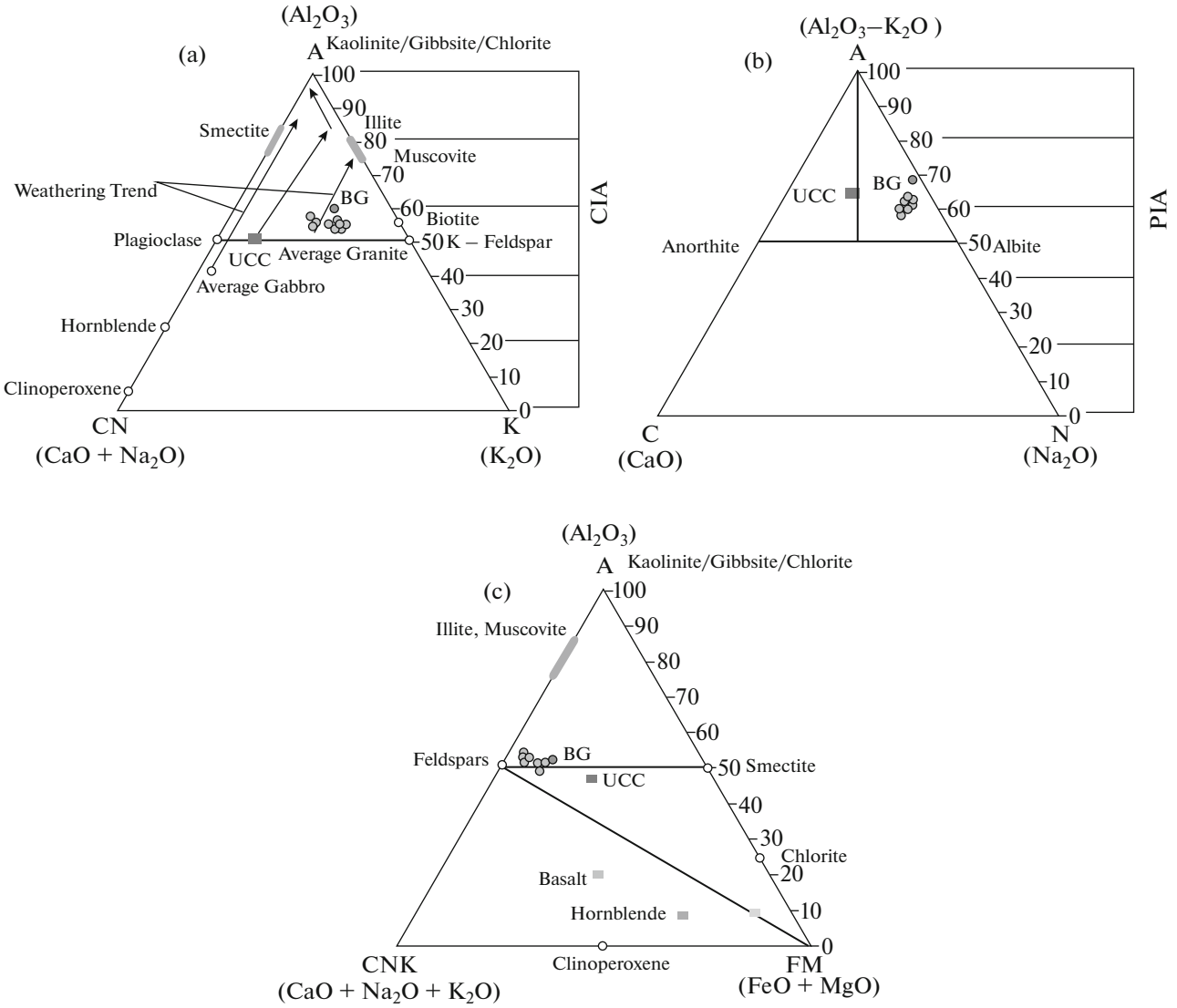

Fig. 5. Ternary plots (a) Major element compositions of sediment samples plotted as molar proportions on an Al_2O_3–(CaO + Na_2O)–K_2O (A–CN–K) diagram (Arrow indicate the weathering trend of the sediments, the scale showing the chemical index of alteration (CIA) is shown at the right side); (b) Major element compositions of sediment samples plotted as molar proportions on an (Al_2O_3–K_2O)–(CaO)–Na_2O (A–C–N) diagram (The scale showing the plagioclase index of alteration (PIA) is shown at the right side); (c) Major element compositions of sediment samples plotted as molar proportions on an Al_2O_3–(CaO + Na_2O + K_2O)–(Fe_2O_3 + MgO) (A–CNK–FM) diagram. All the data were compared with Bundelkhand granite (data after Pati et al., 2015) and UCC (data from Rudnick and Gao, 2003).

chemical weathering intensifies (Nesbitt and Young, 1984). In the A–CN–K plot, the studied samples plot just above the plagioclase tie line with values ranging between 55 and 56 and the CIA value ranges from 54–57 (Fig. 5a). The sediment samples of the Khurar River are close to the average granite and the Bundelkhand granite in the A–CN–K plot, suggesting that the weathering is low and very little plagioclase is transformed into clay. The sediments in general show parallelism to A–CN line and clustering of all the sediments is in a narrow field away from the A–CN line and close to A–K boundary suggesting continuous weathering and mobilization of Ca and Na. It implies that source area for sediments had undergone low to moderate chemical weathering. The CIA of the sediment samples >50 (UCC ~ 50) clearly suggests that the sediment has experienced low to moderate chemical weathering.

A–C–N Diagram

Molar proportions of Al_2O_3 (minus Al associated with K), CaO* and Na_2O was plotted in the A–C–N diagram of Fedo et al. (1995) to monitor the trend of plagioclase weathering in the studied sediments (Fig. 5b). Quantitative measure of plagioclase weathering was

estimated by calculating the PIA defined as $[(Al_2O_3-K_2O)/(Al_2O_3+CaO^*+Na_2O-K_2O)] \times 100$ and is presented in Table 1. Similar to the A–CN–K diagram (Fig. 5a), the plagioclase weathering trend of most of the studied sediments fall on a single line and indicate that the plagioclases in the parent rocks are relatively low to moderately weathered. However, with increasing PIA values, the sediments display low CaO* values and plot close to the Al_2O_3 apex of the triangle. With increasing PIA values, sediments are depleted in Na_2O and enriched in Al_2O_3 indicating the presence of clay minerals. This suggests that increasing chemical weathering in the sediments gradually reduces anorthite and enriches secondary aluminous clay minerals. The studied sediments fall on a linear trend and indicate that they are the weathering products of albite enriched parent material. The PIA values of the studied sediments range between 58 and 64. The PIA values are consistent with the CIA values and suggest that the sediments of Khurar River undergone low to moderate plagioclase weathering. The PIA values are comparable to calculated values of the CIW i.e. chemical index of weathering suggested by Harnois (1988), where CIW is defined as $[Al_2O_3/(Al_2O_3 + CaO^* + Na_2O)] \times 100$ in molar proportions and Cao* is defined as CaO in silicate fractions only (Table 2). In order to establish a relationship between the calculated indices of chemical weathering and elemental ratios, scatter plots of CIA vs. Al/Na, Al/K, Ti/Na, K/Na and Rb/K were used as proxies for intensities of chemical weathering.

A–CNK–FM Diagram

In A–CNK–FM triangular diagram (after Nesbitt and Young, 1984; Nesbitt and Wilson, 1992), the points representing sediment samples lie much closer to the feldspars and indicate relatively lower abundance of kaolinite (Fig. 5c). The studied samples occur above the feldspars-FM join and indicate low abundance of $CaO + Na_2O + K_2O$ in the samples. The trend of the sediments suggests that $CaO + Na_2O + K_2O$ and $Fe_2O_3 + MgO$ components are leached in preference to Al_2O_3 with increasing chemical weathering. This also suggests that feldspars and mafic minerals are weathered to form secondary clay minerals with increasing sediment–water interaction.

Trace Elements Geochemistry

The results of the trace element analysis for the sediments of the Khurar River are listed in Table 2 and the same has been compared with the data obtained from the Bundelkhand granite (BG) (after Pati et al., 2015), UCC (Rudnick and Gao, 2003). The trace elements such as Ba, Cr, Rb, Sr and Zr are abundant in the sediment samples and they show significant scatter within the studied samples. The concentrations of Ba (603 to 824 ppm), Cr (7 to 66 ppm), Rb (142 to 178 ppm), Sr (115 to 157 ppm) and Zr (51 to 193 ppm) vary significantly (Table 2). Zn contents ranges from 2 to 4 ppm. However, Zn is high in some samples (K1, K2 and K15) probably due to anthropogenic activities such as agriculture. High Ba may be derived from the K-feldspar megacrysts (Nemec, 1975). The barium and rubidium contents (Ba from 603 to 824 ppm and Rb 142 to 178 ppm) in the studied sediments are attributed to the presence of K-feldspar and phyllosilicates. The Rb and Ba cations with relatively large ionic radii may be fixed by preferential exchange and adsorption on clays (Nesbitt et al., 1980; Wronkiewicz and Condie, 1989). The low content of clay in the studied sediments negates this possibility. The Th, Nb, Zr and Y have strong negative correlation with SiO_2 and more or less strong positive correlation with other oxides such as Al_2O_3, TiO_2, Fe_2O_3, MgO, CaO, Na_2O and P_2O_5 (Table 3). The behavior of trace elements during sedimentary processes is complex due to factors including weathering, physical sorting, adsorption, provenance, digenesis and metamorphism (Nesbitt et al., 1980; Taylor and Mclennan, 1985; Wronkiewicz and Condie, 1989). The trace element data in the studied sediments show some variation in comparison to the UCC and the Bundelkhand granite (BG) because of fractionation of some elements during weathering, physical sorting and adsorption during sedimentation. In general, Ba, Cr and Sr are enriched, and Rb and Zr are depleted in comparison to Bundelkhand granite (the source rock) in the studied sediments. In the studied sediments, the high field strength elements such as Th, Nb, Zr and Y, normally immobile during sedimentary processes in comparison to other trace elements, show their concentrations (except Th at some stations) below the UCC.

Rare Earth Element Geochemistry

Total rare earth elements concentrations in the Khurar River sediments vary between 45 and 215 ppm (Table 2). There is a significant increase in LREE compared to HREE with high LREE/HREE ratios (5.87 to 10.46) in the studied sediments. River borne sediments usually have REE pattern that are strongly depleted in HREE (Sholkovitz, 1988). The Khurar River sediments show strongly LREE fractionated pattern due to weathering and selective sorting, adsorption during transportation in comparison to source rock BG as illustrated in Figs. 9a, 9b. The LREE enrichment in the sediment samples are also evident by high (La/Yb)N ratios (ranging from 1.33 to 3.24). In contrast, HREE shows less fractionation as seen by the low (Gd/Yb)N ratios (0.48 to 0.84) in the studied sediments. Interestingly the (La/Yb)N ratio in granitic source rocks i.e. Bundelkhand granite is also low 0.87 compared to river sediment samples indicating fractionation of REE during weathering process. A significant feature of the Chondrite-normalized REE pat-

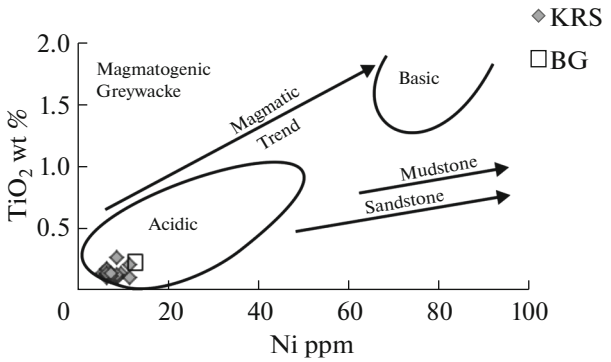

Fig. 6. TiO_2 vs. Ni bivariate plot for the Khurar River sediments (fields after Floyd et al., 1989) compared with Bundelkhand granite (BG) (data after Pati et al., 2015).

tern of Khurar River sediments is the presence of very weak positive Eu-anomaly (avg. samples also show the same in Fig. 9b) and trend of the sediments samples is more or less parallel with the source rock (Figs. 9a, 9b). A close examination of REE suggests that the bulk of HREE are same as the parent rock.

DISCUSSION

Provenance

The intensity and duration of weathering in siliciclastic sediments can be determined through examining the relationships among alkali and alkaline earth elements (Nesbitt and Young, 1982). Since the upper crust is dominated by the presence of feldspars and volcanic glass (Nesbitt and Young, 1982, 1984), the dominant process during chemical weathering and soil formation is the degradation of labile feldspars from source rocks. The chemical signatures are ultimately transferred to sedimentary records and they serve as a useful means for monitoring the original composition even after weathering. Any provenance interpretation of mineralogical, chemical, or detrital-geochronology datasets requires quantitative understanding of hydraulically controlled compositional variability (Garzanti et al., 2010). As the particle size of the bed load sediments of the Khurar River are very coarse to coarse-grained and they have been transported by the rolling process, the effect of hydraulics is constrained here.

The position of the samples in the A–CN–K (Fig. 5a) and A–C–N (Fig. 5b) compositional space suggests that most of the sediments are derived from felsic source which is Bundelkhand granite in the catchment area of the river basin. In the A–CNK–FM compositional space also (Fig. 5c), the sediments plot near to the feldspar apex suggesting the presence of felsic minerals. The sediments of the river comprise quartz, plagioclases and K-feldspars are presented in the compositional triangle of feldspars, kaolinite and smectite near to the feldspar along the feldspar–smectite line in the A–CNK–FM ternary plot. The sediment samples fall much closer to the feldspars and indicate relatively very low abundance of kaolinite. With increasing sediment–water interaction, feldspars and mafic minerals in river sediments are chemically weathered to form secondary clay minerals (kaolinite) (Roy et al., 2012; Verma et al., 2012). The absence of clay minerals in the sediments is consistent with the low to moderate weathering of the Bundelkhand granite before it is derived as sediments and deposited in the Khurar River.

The depletion of MnO and P_2O_5 together with the enrichment of CaO content suggests the alteration of plagioclase as a result of low to moderate weathering and recycling. The enrichment of SiO_2 in comparison to BG suggests dilution of unstable oxides during weathering. The ratio of Al_2O_3/TiO_2 is considered as a good indicator of provenance for sedimentary rocks, in particular, if the source is igneous in nature (Hayashi et al., 1997). The average value of this ratio calculated for the Khurar River bed load samples is 66.83, compatible with a granitic source i.e. Bundelkhand granite ($Al_2O_3/TiO_2 = 57.82$) (data after Pati et al.2015). In TiO_2 vs. Ni bivariate plot (following Floyd et al., 1989), all the points fall in the acidic field (Fig. 6) suggesting felsic source to the studied sediments as expected.

Several trace elements and REE are considered to be useful in discriminating source rock composition and tectonic setting due to their relatively low mobility during sedimentary processes and their short residence times in sea water (Taylor and MacLennan, 1985). These elements are probably transferred quantitatively in clastic sediments during weathering and transportation, reflecting signatures of the parent rock (Bhatia and Crook, 1986). Transition metal elements (Co, Cu, Ni and V) are relatively immobile through weathering, they are well-suited in magmatic processes and therefore, they are highly concentrated in mafic and ultramafic rocks than felsic igneous source rocks. They are considered to be transported completely in terrigenous component of sediments and thus, mirror the chemistry of their source rocks (McLennan el al., 1990). The high values of Ba and Rb in the studied sediments are attributed to the presence of K-feldspar and phyllosilicates suggesting felsic source for them as expected. Ba and Co are largely contained in K-bearing and ferromagnesian minerals, respectively and the relative contribution of mafic/felsic source can be reflected by the Ba/Co ratio (Taylor and McLennan, 1985). The elevated Ba and depleted Co contents in the bed load sediments of the Khurar River suggests the dominance of K-feldspars and poor presence of the ferromagnesian minerals in the source rock. The higher Ba/Co ratio (Table 2) is an indication of sediments derived from weathered felsic-granitic source rock (AK Arish and El-Gohary, 2008).

The High field strength elements Zr, Nb, Hf, Y, Th, and U are preferentially partitioned into melts

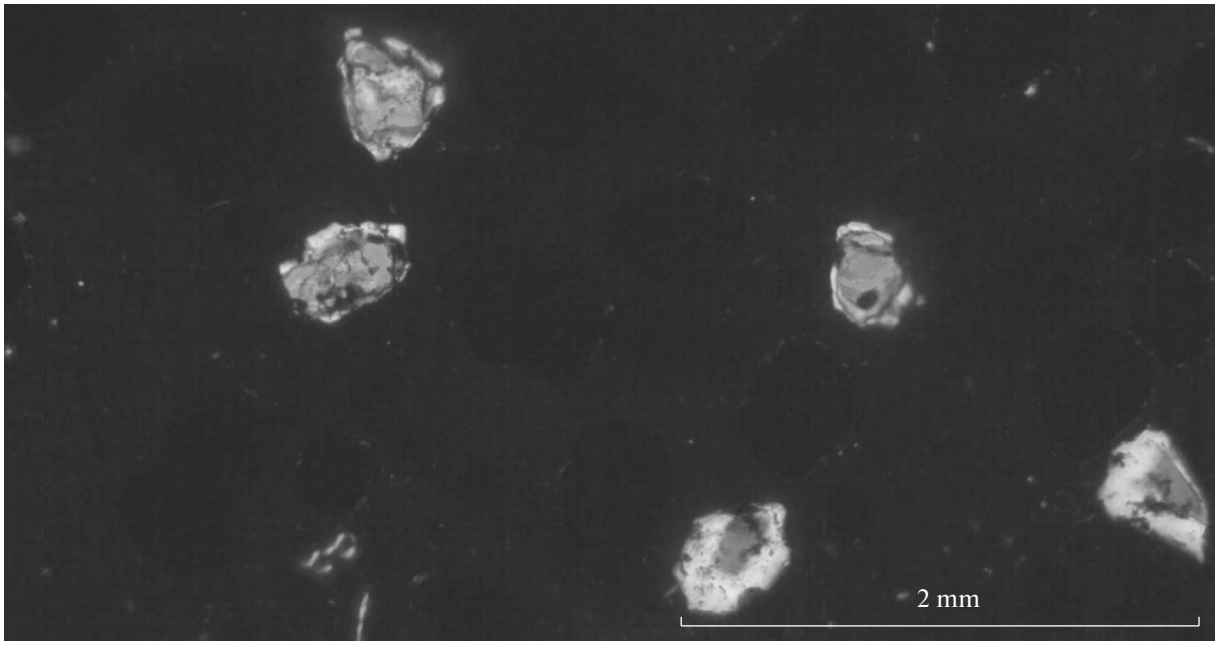

Fig. 7. Photomicrograph showing the presence of mineral zircon separated from the heavy liquid separation. Note zoning in all the zircon minerals.

through crystallization (Feng and Kerrich, 1990) and therefore, these elements are enriched in felsic rather than mafic rocks. Along with REE, HFSE (High field strength elements) are thought to specify compositions of provenances. A possible explanation for the HFSE depletion is a heavy mineral effect caused by fractionation of heavy minerals by sedimentary sorting processes (e.g. McLennan et al., 1993). The strong negative correlative between SiO_2 and Zr suggests the presence of zircon mineral in the sediment samples. The presence of zircon is also recorded during the heavy mineral analysis of the sediment samples (Fig. 7). The La/Th vs. Th/Yb and Th/Co vs. Zr/Co plots are useful in differentiating between felsic and mafic source rocks (Bhatia and crook, 1986; Borges et al., 2008; Akarish and El-Gohary, 2008). In them (Figs. 8a, 8b), the studied samples show high La/Th and high Th/Co ratios indicating felsic character of source rock.

The REE and Th are fairly helpful to deduce crustal compositions because their distribution is not significantly affected by secondary processes such as diagenesis and metamorphism and is less affected by heavy mineral fractionation than that for elements such as Zr, Hf and Sn (Bhatia and Crook, 1986). REE and Th contents are higher in felsic than mafic igneous source rocks and their weathering products, Further, Eu/Eu*, (La/Lu)N, Th/Co and La/Co ratios are significantly unlike in mafic and felsic source rocks and may be useful in constraining the provenance of sedimentary rocks (Cullers, 1988). The Eu/Eu*, (La/Lu)N, Th/Co and La/Co ratios of the studied sediment samples are comparable with those sediments derived

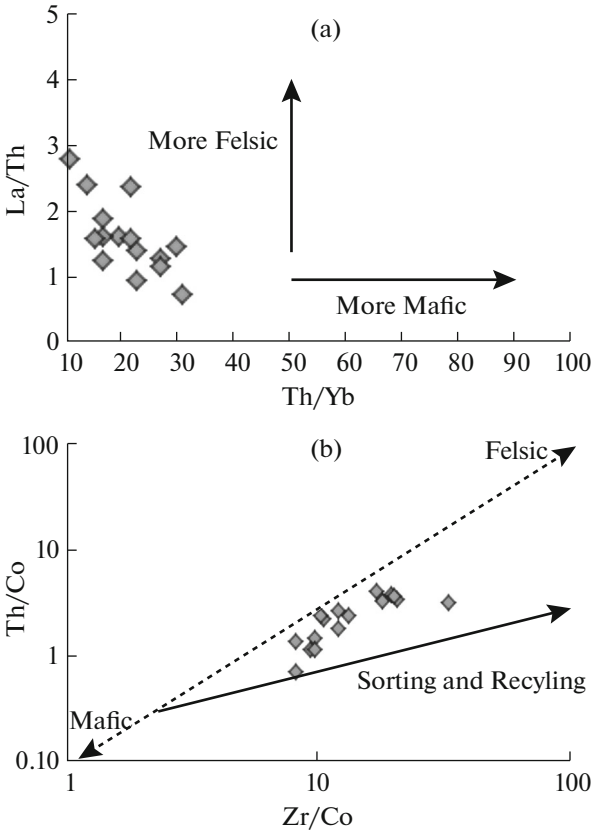

Fig. 8. (a) La/Th vs. Th/Yb plot showing felsic vs. mafic character (McLennan et al., 1980). (b) Th/Co vs. Zr/Co plot show mafic–felsic character and recycling (McLennan et al., 1993).The dashed line indicates compositional difference, and deviation from this trend (solid line) represents sedimentary effects from sorting and recycling.

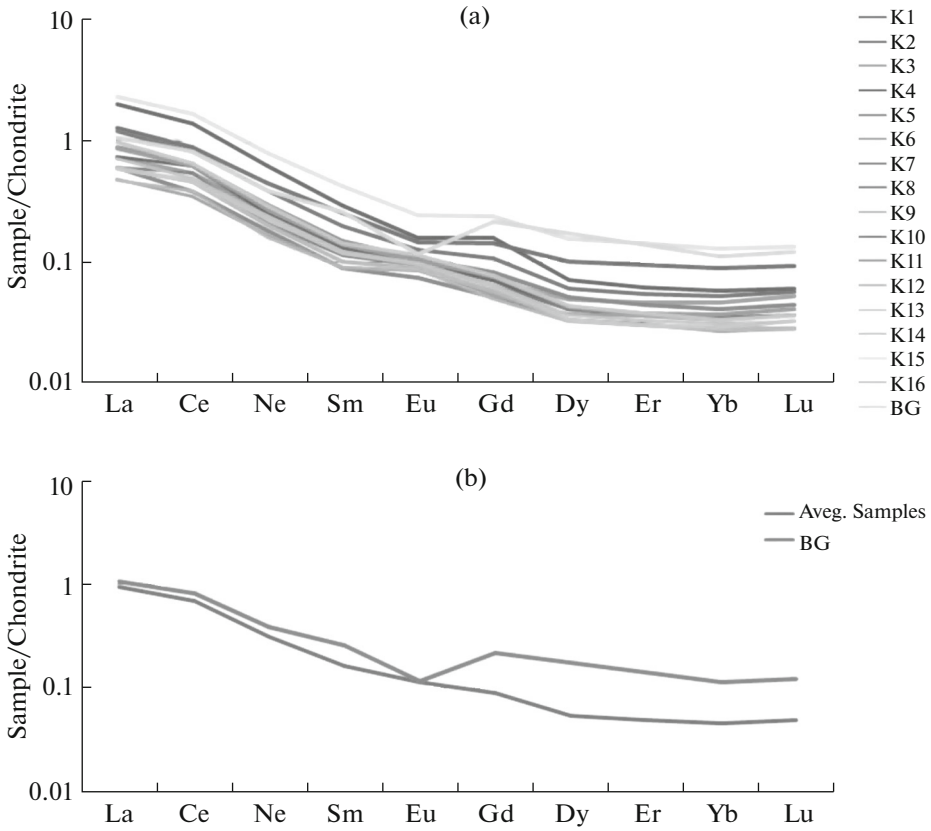

Fig. 9. Chondrite-normalized REE patterns (after McDonough and Sun, 1995) (a) individual samples, (b) average value of all the samples of Khurar River sediments.

from felsic source rocks rather than mafic source rocks (Table 2). The Eu anomaly is retained as the more conservative provenance proxy (McLennan et al., 1993; Cullers, 2000). The Eu anomaly values of all the sediment samples are consistent with its value in the granitic source occurring in the provenance (Table 2). This also shows the low fractionation of the plagioclase feldspar during weathering and sedimentation. Under the prevailing chemical weathering conditions in the catchment areas of the Khurar River, the bulk of the REE were derived by the weathering of felsic minerals present in the granite.

The relative REE patterns and Eu anomaly size are utilized to deduce sources of sedimentary rocks (Taylor and McLennan, 1985). Mafic rocks contain low LREE/HREE ratios and tend not to contain Eu anomalies, whereas more felsic rocks usually contain high LREE/HREE ratios and negative Eu anomalies (Cullers and Graf, 1984). The high LREE/HREE ratios, but positive Eu anomaly (Figs. 9a, 9b) in the studied sediments are due to the granitic source and low fractionation of plagioclase during weathering.

The extent of LREE fractionation in the sediment samples is also evident by high (La/Yb)N ratios (ranging from 1.33 to 3.24). In contrast, HREE shows less fractionation as seen by the low (Gd/Yb)N ratios (0.48 to 0.84). Interestingly, the (La/Yb)N ratio (0.87) in the granitic source rock (data after Pati et al. 2015) is also low compared to river sediments indicating some fractionation of REE during weathering process.

Weathering and Climate

Chemical weathering affects the mineralogy and major, trace and REE geochemistry of the siliciclastic sediments. Depending on the solubility and ion potential, labile cations (Na, K, Ca, Rb) are leached in preference to insoluble hydrolysates (Ti, Al) (Nesbitt and Young, 1982; Smykatz-Kloss et al., 2004). However, it has been argued that both K and Rb are incorporated into clay minerals by adsorption and cation exchange during initial weathering of fresh rocks (Nesbitt et al., 1980) and K is preferentially leached compared to Rb with increasing weathering, (Wronkiewicz and Condie, 1989). Thus, the ratios of Al/Na, Ti/Na, Al/K, Al/Ca and Rb/K gradually increase with increasing chemical weathering (Fig. 10). Similarly, the ratio of K/Na suggests the abundance of K-feldspars compared to Na-plagioclases. As K-feldspars are relatively more resistant to weathering compared to Ca-Na feldspars, higher K/Na suggests higher degree of chemical weathering. The CIA values

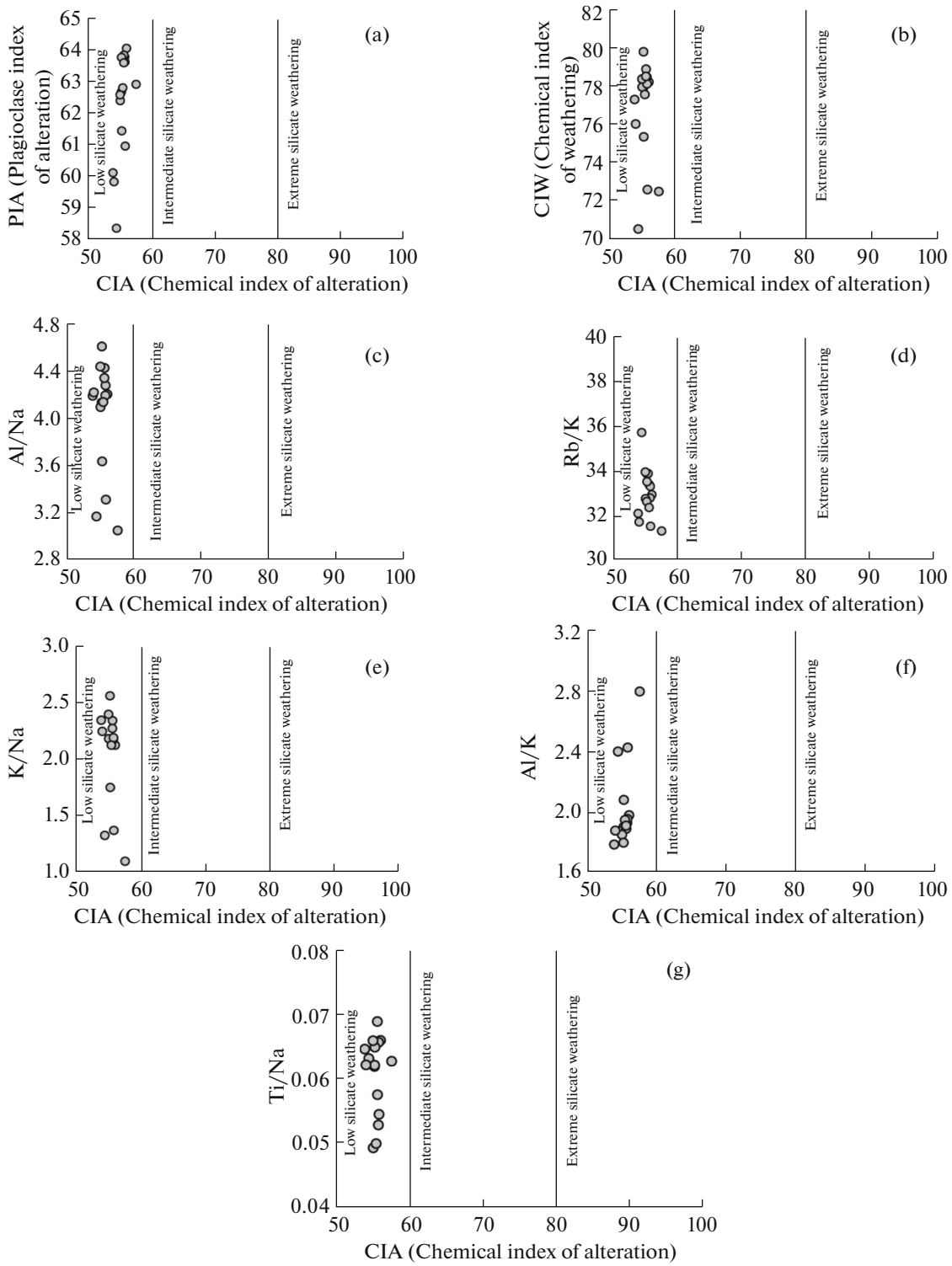

Fig. 10. Scatter plots of chemical index of alteration (CIA) vs. PIA, CIW, Al/Na, Rb/K, K/Na, Al/K and Ti/Na for the Khurar River sediments.

also have significant relationship with ratios of K/Na and Al/K (Fig. 10). The CIA and the K/Na and Al/K values are consistent with the low to moderate weathering regime in the river catchment. Further, the enrichment of CaO from the BG looks related to its precipitation in the sediments similar to other rivers such as Bhima, Krishna and Godavari of India (also see Das and Krishnaswami, 2007; Vuba et al., 2015).

Table 4. Chemical index of alteration (CIA), plagioclase index of alteration (PIA), chemical index of weathering (CIW) and molar ratios of Al/Na, Al/K, K/Na, Ti/Na and Rb/K of the Khurar River sediments

	K1	K2	K3	K4	K5	K6	K7	K8	K9	K10	K11	K12	K13	K14	K15	K16
Al/Na	3.17	3.31	4.13	4.20	4.19	4.09	4.42	4.28	4.14	3.64	4.44	4.61	4.19	4.22	3.05	4.34
Al/K	2.40	2.43	1.90	1.98	1.93	1.88	1.89	1.96	1.95	2.08	1.86	1.80	1.79	1.88	2.80	1.92
K/Na	1.32	1.36	2.17	2.12	2.17	2.17	2.34	2.18	2.12	1.74	2.39	2.55	2.34	2.24	1.09	2.27
Ti/Na	0.06	0.05	0.06	0.07	0.05	0.05	0.06	0.07	0.05	0.06	0.07	0.06	0.06	0.06	0.06	0.07
Rb/K	35.73	31.56	33.90	32.96	32.82	32.78	33.41	33.33	33.91	33.54	33.97	32.66	32.13	31.75	31.34	32.39
CIW	70.57	72.62	77.94	78.23	78.49	77.97	78.90	78.13	77.58	75.37	78.39	79.80	77.32	76.04	72.53	78.52
CIA	54.55	55.91	55.31	56.11	55.83	55.13	55.70	55.86	55.52	55.36	55.11	55.32	54.01	54.17	57.59	55.69
PIA	58.33	60.95	62.66	64.06	63.79	62.39	63.84	63.62	62.80	61.43	62.58	63.77	60.10	59.81	62.91	63.60

The low to moderate weathering in the source area and physical sorting looks responsible for the low to moderate fractionation of trace elements also in the studied sediments compared to BG. The high Zn content in some samples (K1, K2 and K15) may be due to anthropogenic activities such as agriculture.

The weathering history of the source of siliciclastic sediments can be determined through quantitative estimation of the chemical weathering of silicates such as the calculated values of chemical index of alteration (CIA), plagioclase index of alteration (PIA) and chemical index of weathering (CIW) (Nesbitt and Young, 1982; Fedo et al., 1995). This is suggested by increasing values of CIA, PIA, CIW and the trend showing preferential leaching of $CaO + Na_2O + K_2O$ and $Fe_2O_3 + MgO$ relative to Al_2O_3. The intensity of chemical weathering and the composition of siliciclastic sediments are controlled by the climate of the area (Sensarma et al., 2008). The variation in CIA, PIA and CIW values may be due to the different concentrations of alumina and the low values of them in the Khurar River sediments suggest that the low to moderate chemical weathering was effective in the river catchment. The CIA values are in good agreement with those of PIA and CIW and show a linear relationship and covariance (Table 4) (e.g. Roy et al., 2012). The linear relationship and covariance among the CIA, PIA and CIW values (Fig. 10) suggest that they followed the same trend during weathering. The weathering trend might have been influenced by the past and present climates prevailing in the river catchment.

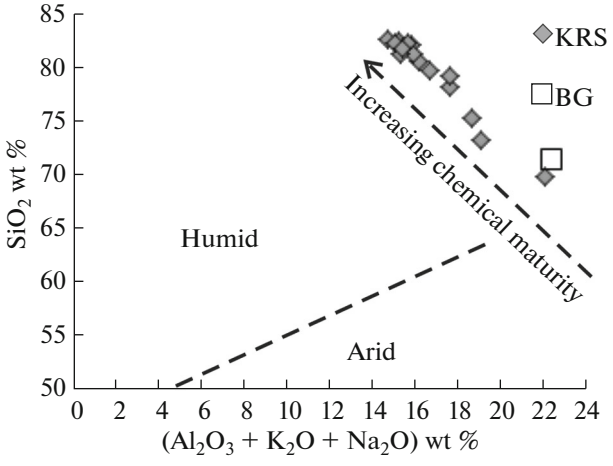

Fig. 11. SiO_2 vs. $(Al_2O_3 + K_2O + Na_2O)$ plot discriminating climate and chemical maturity of Khurar River sediments (after Suttner and Dutta, 1984). Note that all the sediments fall in the humid climate field.

In humid climatic region, chemical weathering exceeds the physical weathering whereas in arid climate physical weathering exceeds chemical (Suttner and Dutta, 1986). The sediment samples of the Khurar River can be taken as an indicator of the past weathering influenced by the prevailing climate. The predicted climate is well depicted in Fig. 11, where the samples are plotted in the humid climate field indicating moderate chemical weathering and low physical weathering. The present-day climate of the area under investigation is sub-humid. It is presumed that a similar climate resulted low to moderate weathering of the Bundelkhand granite occurring in the river catchment.

CONCLUSIONS

The results and discussion of the present study lead to the following conclusions:

(1) The bed-load sediments derived from the granitic source in a small river within the very coarse to coarse grain size range are arkosic in composition.

(2) The sediments are enriched in SiO_2 in comparison to the source because of removal of unstable elements during weathering and entrainment.

(3) The CIA, PIA and CIW values of the sediments suggest low to moderate weathering of granite either in the sub-humid or similar climatic conditions.

(4) These sediments show higher values of Rb and Pb and lower values of Cr, Co, Cu and Ni than UCC due to less varied source of the studied sediments than that.

(5) The sediments show HREE depletion with a weak positive Eu anomaly due to low fractionation of the plagioclase feldspars during weathering.

ACKNOWLEDGMENTS

The authors are thankful to the Head of the Department of Geology, Banaras Hindu University for providing working facilities. The financial support from the University Grant Commission, New Delhi to SK and SS for carrying out this research work is gratefully acknowledged. We are thankful to the Director Wadia Institute of Himalayan Geology for analytical support. Dr. Kuldeep Prakash is acknowledged for his help during the preparation of this manuscript. We acknowledge the help received by the journal reviewer and the editor.

REFERENCES

A. I. M. Akarish and A. M. El–Gohary, "Petrography and geochemistry of lower Paleozoic sandstones, East Sinai, Egypt: Implications for provenance and tectonic setting," J. Afri. Ear. Sci., **52**, 43–54 (2008).

M. R. Bhatia and K. A. W. Crook, "Trace element characteristics of graywackes and tectonic setting discrimination of sedimentary basins," Contrib. Mineral. Petrol, **92**, 181–193(1986).

J. B. Borges, Y. Huh, "Petrography and chemistry of the bed sediments of the Red River in China and Vietnam: provenance and chemical weathering," Sedimentary Geol. **194**, 155–168 (2007).

J. B. Borges, Y., Huh, S. Moon, H. Noh, "Provenance and weathering control on river bed sediments of the eastern Tibetan Plateau and the Russian Far East," Chem. Geol. **254**, 52–72 (2008).

K. C. Condie, "Another look at the rare earth elements in shales," Geochim. Cosmochim. Acta, **35**, 2527–2531 (1991).

R. L. Cullers, "Mineralogical and chemical changes of soil and stream sediment formed by intense chemical weathering of Danburg granite, Georgia, USA," Lithos, **21**, 301–314 (1988).

R. L. Cullers, "The geochemistry of shales, siltstones, and sandstones of Pennsylvanian–Permian age Colorado, U.S.A.: Implications for provenance and metamorphic studies," Lithos, **51**, 181–203 (2000).

R. L. Cullers and J. Graf, "Rare earth element in igneous rocks of the continental crust: intermediate and silicic rocks," *Rare Earth Geochemistry,* Ed. by H. Henderson (Elsevier, Amsterdam, 1984), pp. 275–316.

A. Das and S. Krishnaswami, "Element geochemistry of river sediments from the Deccan Traps, India: Implications to sources of elements and their mobility during basalt—water interaction," Chem. Geol., **242**, 232–254 (2007).

C. M. Fedo, H. W. Nesbitt, and G. M. Young, "Unraveling the effects of potassium metasomatism in sedimentary rocks and paleosols, with implications for paleoweathering conditions and provenance," Geology **23**, 921–924 (1995).

R. Feng and R. Kerrich, "Geochemistry of the fine grained clastic sediments in the Archean Abitibi greenstone belt, Canada: Implications for provenance and tectonic setting," Geochim. Cosmochim. Acta, **54**, 1061–1081 (1990).

P. A. Floyd, J. A. Winchester, and R. G. Park, "Geochemistry and tectonic setting of Lewisianclasticmeta–sediments from the Early Proterozoic Loch Maree Group of Gairloch, N.W. Scotland," Precambrian Res. **45**(1–3), 203–214(1989).

J. Gaillardet, B. Dupré, P. Louvat, and C. J. Allègre, "Global silicate weathering and CO_2 consumption rates deduced from the chemistry of large rivers," Chem. Geol., **159**, 3–30(1999).

E. Garzanti, C. France–Lanord, P. Censi, and V. Galy, "Mineralogical and chemical variability of fluvial sediments. 1. Bed–load sand: Ganga–Brahmaputra, Bangladesh," Ear. Planet. Sci. Lett., **299**, 368–381 (2010).

K. Hayashi, H. Fujisawa, H. D. Holland, H. Ohmoto, "Geochemistry of ~1.9 Ga sedimentary rocks from northeastern Labrador, Canada," Geochim. Cosmochim. Acta **61**, 4114–4137 (1997).

L. Harnois, "The CIW index; a new index of weathering," Sedimentary Geol. **55**, 319–322 (1988).

M. M. Herron, "Geochemical classification of terrigenous sand and shale from core or log data," J. Sediment. Petrol. **58**, 820–829 (1988).

S. Kanhaiya and B. P. Singh, "Spatial variation of textural parameters in a small River: An Example from Khurar River, Khajuraho, Chhaterpur District, Madhya Pradesh, India," Glob. J. Earth Sci. Eng., **1**, 34–42 (2014).

P. Kaur, A. Zeh, and N. Chaudhri, "Characterisation and U–Pb–Hf isotope record of the 3.55 Ga. felsic crust from the Bundelkhand craton, northern India," Precambrian Res. **255**, 236–244 (2014).

P. P. Khanna, N. K. Saini, P. K. Mukherjee, and K. K. Purohit, "An appraisal of ICP–MS technique for determination of REEs: long term QC assessment of Silicate rock analysis," Himal. Geol., **30**(1), 95–99 (2009).

W. F. McDonough and S. S. Sun, "The composition of the Earth" Chem. Geol. **120**, 223–253 (1995).

S. M. McLennan, "Rare earth element in sedimentary rocks: Infuences of provenance and sedimentary processes," Geochemistry and Mineralogy of Rare Earth Elements, Ed. by B. R. Lipin and G. A. McKay, (Min. Soc. Am., 1989), pp. 169–200 (1989).

S. M. McLennan, S. Hemming, D. K. McDaniel, and G. N. Hanson, "Geochemical approaches to sedimentations, provenance and tectonics," Geol. Soc. Am. Spec. Papers, **284**, 21–40 (1993).

S. M. McLennan, S. R. Taylor, M. T. McCulloch, and J. B. Maynard, "Geochemical and Nd–Sr isotopic composition of deep–sea turbidities: crustal evolution and plate tectonic associations," Geochim. Cosmochim. Acta, **54**, 2015– 2050 (1990).

D. Nemec, "Barium in K–feldspar megacrysts from granitic and syenitic rocks of the Bohemian Massif," Tschermaks Mineral. Petrogr. Mitt., **22**, 109–116 (1975).

H. W. Nesbitt, "Petrogenesis of siliciclastic sediments and sedimentary rocks, in Lentz D.R. ed., Geochemistry of sediments and sedimentary rocks: evolutionary consid-

eration to mineral deposits forming environments Geological association of Canada," Geo text, **4**, 39–51(2003).

H. W. Nesbitt and R. E. Wilson, "Recent chemical weathering of basalts," Am. J. Sci. **292**, 740–777 (1992).

H. W. Nesbitt and G. M. Young, "Early Proterozoic climates and plate motion inferred from major element chemistry of lutites," Nature, **299**, 715–717 (1982).

H. W. Nesbitt and G. M. Young, "Prediction of some weathering trends of plutonic and volcanic rocks based on thermodynamic and kinetic considerations," Geochim. Cosmochim. Acta **48**, 1523–1534 (1984).

H. W. Nesbitt and G. M. Young, "Petrogenesis of sediments in the absence of chemical weathering: effects of abrasion and sorting on bulk composition and mineralogy" Sedimentology, **43**, 341–358 (1996).

H. W. Nesbitt, G. Markovics, and R. C. Price, "Chemical processes affecting alkalis and alkaline earths during continental weathering," Geochim. Cosmochim. Acta **44**, 1659–1666 (1980).

P. Oliva, J. Viers, and B. Dupre, "Chemical weathering in granitic environments," Chem. Geol., **202**(3), 225–256 (2003).

J. K. Pati, W. U. Reimold, A. Greshake, R. T. Schmitt, C. Koeberl, P. Pati, and K. Prakash, "Pseudotachylitic breccia from the Dhala impact structure, north–central India: texture, mineralogy and geochemical characterization," Tectonophysics, **649**, 18–32 (2015).

F. J. Pettijohn, P. E. Potter, and R. Siever, *Sand and Sandstones*, (New York, Springer–Verlag, 1972).

K. K. Purohit, N.K. Saini, and P. P. Khanna, "Geochemical description pattern of heavy mental abundance in intermontane Pinjaur Dun, Sub–Himalaya," Him. Geol., **31**(1), 29–34 (2010).

P. D. Roy, J. L. Arce, R. Lozano, M. P. Jonathan, E. Centeno, and S. Lozano, "Geochemistry of late quaternary tephra–sediments sequence from north–eastern basin of Maxico (Maxico): implications to tephrochronology, chemical weathering and provenance," Revista Mexicana Ciencias Geológicas, **29** (1), 24–38 (2012).

R. L. Rudnick and S. Gao, "Composition of the continental crust," Treatise Geochem. **3**, 1–64 (2004).

L. Saha, N. C. Pant, J. K. Pati, D. Upadhyay, J. Berndt, A. Bhattacharya, and M. Satynarayanan, "Neoarchean high–pressure margarite–phengiticmuscovite–chlorite corona mantled corundum in quartz–free high–Mg, Al phlogopite–chlorite schists from the Bundelkhand craton, north central India," Contrib. Mineral. Petrol. **161**, 511–530 (2011).

A. Sarkar, J. R. Trivedi, K. Gopalan, P. N., Singh, B. K. Singh, A. K. Das, and D. K. Paul, "Rb–Sr Geochronology of the Bundelkhand granitic complex in the Jhansi–Babina–Talbehat sector, U.P.," Ind. J. Ear. Sci., CEISM seminar volume, 64–72(1984).

S. Sensarma, V. Rajamani, and J. K. Tripathi, "Petrography and geochemical characteristics of the sediments of the small river Hemavati, South India: implications for provenance and weathering processes," Sedimentary Geol. **205**, 111–125 (2008).

L. Shapiro and W. W. Brannock, "Rapid analysis of silicate, carbonate and phosphate rocks," U.S. Geol. Surv. Bull., **48**, 49–55 (1962).

A. Sharma, S. Sensarma, K. Kumar, P. P. Khanna, and N. K. Saini, "Mineralogy and geochemistry of the Mahi River sediments in tectonically active western India: Implications for Deccan large igneous province source, weathering and mobility of elements in a semi-arid climate," Geochim. Cosmochim. Acta **104**, 63–83 (2013).

E. R. Sholkovitz, "Cycling of dissolved rare earth Elements in Chesapeake Bay," Global Biogeochemical Cycles **2** (2), 157—176 (1988).

A. L. Stork, D.K. Smith, and J. B. Gill, "Evaluation of geochemical reference standards by X–ray fluorescence analysis," Geostand. Newslett. **11**, 107–113(1987).

L. J. Suttner and P. K. Dutta, "Alluvial sandstones composition and paleoclimate, I. Framework mineralogy". J. Sedimentary Petrol. **56**, 329–345(1986).

N. K. Saini, P. K. Mukherjee, M. S. Rathi, and P. P. Khanna, "Evaluation of energy–dispersive x–ray fluorescence spectrometry in the rapid analysis of silicate rocks using pressed powder pellets," X–Ray Spectrom. **29**, 166–172 (2000).

S. R. Taylor and S. M. McLennan, *The Continental Crust: Its Composition and Evolution* (Blackwell, London, 1985).

M. Verma, B. P. Singh, A. Srivastava, and M. Mishra, "Chemical behaviour of suspended sediments in a small river draining out of the Himalaya, Tawi River, northern India: implications on provenance and weathering," Himal. Geol. **33**(1), 1–14 (2012).

S. K. Verma, S. P. Verma, P. E. Oliveira, V. K. Singh, and J. A. Moreno, "LA-SF-ICP-MS zircon U–Pb geochronology of granitic rocks from the central Bundelkhand greenstone complex, Bundelkhand craton, India," J. Asian Earth Sci. **118**, 125–137 (2016).

S. Vuba, S. M. Ahamad, and N. R. Anipindi, "Geochemical and mineralogical studies in recent clastic sediments from upper Godavari River in peninsular India," J. Geol. Soc. India **86**, 107–114 (2015).

A. F. White and A. E. Blum, "Effects of climate on chemical weathering in watersheds," Geochim. Cosmochim. Acta **59** (9), 1729–1747 (1995).

G. P. Whitemore, K. A. W. Crook, and D. Johnson, "Grain size control of mineralogy and geochemistry in modern river sediment, New Guinea collision, Papua New Guniea," Sedimentary Geol. **17**, 129–157 (2004).

D. J. Wronkiewicz and K. C. Condie, "Geochemistry and provenance of sediments from the Pongola Supergroup, South Africa: evidence for a 3.0 Ga. Old continental craton," Geochim. Cosmochim. Acta **53**, 1537–1549 (1989).

S. Y. Yang, H. S. Jung, M. S. Choi, and C. X. Li, "The rare earth element compositions of the Changjiang (Yangtze) and Huanghe (Yellow) river sediments," Earth Planet. Sci. Lett. **201**, 407–419 (2002).